

RADIOIMMUNOIMAGING OF NON-SMALL CELL LUNG CANCER WITH ^{111}In - AND $^{99\text{m}}\text{Tc}$ -LABELED MONOCLONAL ANTI-CEA-ANTIBODIES

KALEVI J. A. KAIREMO, HANNU J. ARONEN, KRISTIAN LIEWENDAHL, TIMO PAAVONEN, JORMA J. HEIKKONEN, PEKKA VIRKKUNEN, HELJÄ MÄKI-HOKKONEN, SIRKKA-LIISA KARONEN, ANNA-LIISA BROWNELL and MATTI J. MÄNTYLÄ

Radiolabeled monoclonal anti-CEA antibodies were used for radioimmunolocalization (RIL) of non-small cell lung cancer; in 30 patients with ^{111}In labeled anti CEA F(ab')_2 fragment (BW 431/31) and in 16 with $^{99\text{m}}\text{Tc}$ -labeled intact MoAb (BW 431/26). RIL results were compared with those of other imaging modalities. Paraffin sections from some patients were also studied immunohistochemically using anti-CEA antibody. Patients with ^{111}In labeled MoAB were imaged twice 1–4 days after injection and for image enhancement pulmonary and liver/spleen subtraction were performed. Twenty-seven of 28 primary tumors were positive and metastases were detected in all patients. The total number of lesions was 78 of which 61 (78%) could be detected by RIL. For verification CT was applied to the study of 46 lesions detected by RIL. We found 6 unknown lesions subsequently verified histologically. Using subtraction techniques we detected 9 lesions in 4 patients, later verified as pulmonary metastases, not detected in unprocessed images. Pleural, mediastinal and pericardial lesions were also better delineated in subtracted images than in unprocessed images. Imaging of non-small cell lung cancer with $^{99\text{m}}\text{Tc}$ -labeled MoAB was performed twice 4–24 h after injection. RIL results were compared with other imaging methods; CT US, conventional radiography, and immunohistochemistry. Twelve out of 16 patients with suspected or known lung cancer had positive immunoscintigrams; 19 of 25 lesions could be detected by RIL. There were 5 false positive and 2 true negative findings. Immunoperoxidase (IP) stainings of paraffin sections of the tumours from 7 patients were performed using two different anti-CEA antibodies; BW 431/26 and ZCEA₁. None of the seven tumors examined by immunohistochemistry were negative when stained by BW 431/26, which was the antibody used for immunoscintigraphy.

Received 3 February 1993.

Accepted 14 April 1993.

From the Department of Clinical Chemistry (K. Kairemo, K. Liewendahl, S.-L. Karonen, A.-L. Brownell), Radiology (H. Aronen), Pathology (T. Paavonen), and radiotherapy and Oncology (J. Heikkonen, P. Virkkunen, H. Mäki-Hokkonen, M. Mäntylä), Helsinki University Central Hospital, Helsinki, Finland,

Correspondence to: Dr Kalevi Kairemo, Division of Nuclear Medicine, Department of Clinical Chemistry, Helsinki University Central Hospital, Haartmaninkatu 4, SF-00290 Helsinki, Finland. Presented at the 3rd Scandinavian Symposium on Monoclonal Antibodies in Diagnosis and Therapy of Cancer, October 30–31, 1992, Helsinki, Finland.

The most useful radiological staging methods of primary lung cancer are magnetic resonance imaging (MRI) and computerized tomography (CT) (1–5). Non-specific radionuclide methods have also been used for detecting lung cancer such as gallium-67 scintigraphy (6, 7). Other lung cancer tracers, apparently with clinical utility, are bleomycin-derivative (8) and glucoheptonate (9). Due to its potentially high specificity, radioimmunodetection is predicted to significantly improve the diagnosis of cancer (10–13). Further advancements are expected from the separate administration of antibody and label (14, 15), and from the use of chimeric antibodies (16, 17), anti-antibody enhancement (18, 19) and bifunctional haptens (20, 21).

There are now a few reports on imaging of lung cancer with polyclonal (11) and monoclonal anti-carcinoembryonic antigen (CEA)-antibodies (19, 22–26). Monoclonal antibodies against other pulmonary cancer cell antigens have been produced, and tested in xenograft studies (27–29). The monoclonal antibody 600D11 labeled with ^{131}I was found to be specific for human small cell lung cancer (NCI-H69) and an adenoma cell line (A549) when tested in mouse xenografts (30). Administration of large doses of ^{125}I labeled MoAB 5E8 reacting with glycoprotein gp 160 on human lung cancer cell surfaces were found to inhibit tumor growth (31). SWA 20 MoAb, developed against a tumor-associated cell surface antigen from human small cell carcinoma showed high affinity to small cell carcinomas (32). An interesting experimental approach is the imaging of mediastinal lymph node metastases from lung cancer in dogs with monoclonal antibody against lung cancer antigen using immunolymphoscintigraphy (33). A promising report on imaging of lung cancer with monoclonal antibodies against *c-myc*-oncogene products has been published (34). A number of problems have to receive proper attention when performing immunoscintigraphy (35). One is the relatively low tumor/background ratio, partly a result of accumulation of the tracer in reticuloendothelial cells (RES). Methods for subtracting RES-activity could be important, particularly when using ^{111}In labeled antibody.

The aim of this study was therefore to test a monoclonal anti-CEA $\text{F}(\text{ab}')_2$ fragment and an intact monoclonal anti-CEA antibody, labeled with either ^{111}In or $^{99\text{m}}\text{Tc}$, for the detection of recurrences and metastases in non-parvocellular pulmonary cancer patients. To improve the interpretation of the immunoscintigrams various subtraction techniques were used: pulmonary and liver/spleen subtractions were performed in all cases and the results were compared with those of other radiological methods (conventional radiograph, ultrasound and computerized tomography).

Material and Methods

Patients. Forty-six consecutive patients with histologically verified non-microcellular lung cancer were investigated (36 males, 10 females; aged 43–79 years, average 55) who underwent a regular staging and clinical follow-up program. The selection criteria were suspicion of metastases or recurrence, or an elevated level of CEA in serum at the time of immunoscintigraphy. The lesions in antibody scans were afterwards examined clinically, radiologically and cytologically/histologically when ethically and therapeutically indicated. The study had the permission of the Ethical Committee of the Department of Radiotherapy and Oncology, University of Helsinki.

Radioantibodies. The monoclonal antibody (BW 431/26) was provided by Behringwerke (Marburg, Germany). This

IgG_1 -subclass antibody was labeled with $^{99\text{m}}\text{Tc}$, using a stannous reduction technique as described in detail (36). The labeling efficiency, measured by thin layer chromatography (ITLC SG, Gelman Sciences, Ann Arbor, Mich., USA), was over 98%. The labeling yield tested by the manufacturer was $95.2 \pm 2.6\%$ and the immunoreactivity 80–85% (37). Sixteen patients were studied. Biological half-life (T_b) was also measured as average in 4 patients by taking consecutive blood samples, and counting them for radioactivity, the average was 23.3 h, and thus the effective half-life (T_e) was 4.7 h from the equation $1/T_b = 1/T_{1/2} + 1/T_e$, where $T_{1/2}$ is the physical half-life of $^{99\text{m}}\text{Tc}$ (6.03).

The monoclonal antibody BW 431/31, also provided by Behringwerke AG, is a $\text{F}(\text{ab}')_2$ fragment of an antibody produced against CEA (38). The fragments, to which DTPA-moieties were attached, were labeled with ^{111}In (InCl_3 , Amersham, England). Thirty patients were studied. The labeled efficiency measured by TLC varied from 84–93%, and the immunoreactivity from 85–90% (37).

Serum CEA concentration. The serum CEA concentration was measured by RIA in all patients 0–19 days before administration of antibody (usually on the day of administration). The upper reference limit of the method was $2.5 \mu\text{g/l}$.

Imaging protocol. All the patients were imaged at least twice. $^{99\text{m}}\text{Tc}$ -anti-CEA: The whole body was scanned at 3–5 h and 20–24 h after injection both with planar spot images and whole body images after a single intravenous injection of $^{99\text{m}}\text{Tc}$ -labeled antibody. The antibody radioactivity was 925–1110 MBq per 2 mg of labeled antibody, which was injected in 5 ml of physiological saline after getting the informed consent from the patient. No skin tests were performed, but the general allergy anamnesis was taken into account. The gamma camera (General Electric 500 Maxi) was equipped with a low energy general purpose collimator. The gamma camera was connected to the Star data processing system (Nova computer). Into each scintigram at 3–5 h 1 200 000 counts and at 20–24 h 700 000 counts were collected in matrix size 128×128 . The whole body scanning speed was 10cm/min.

^{111}In -anti-CEA: In the first investigation (20–28 h) whole body imaging was performed with a Siemens Scintiview gamma camera, equipped with a medium energy collimator. Planar spot imaging was performed by collecting 350 000–800 000 counts per image; administered activity was 74–150 MBq. A skin test was performed half an hour before the intravenous administration of tracer. The second imaging study (49–77 h) was performed using a General Electric Maxi 400T camera with SPECT facility. Brain SPECT was performed in 4 cases by collecting 64 35-s frames.

Subtraction methods. In the second imaging phase (20–24 h for $^{99\text{m}}\text{Tc}$ and 49–77 h for ^{111}In) liver and pulmonary perfusion subtraction studies were performed in all patients. The patient was first injected $^{99\text{m}}\text{Tc}$ -labeled

phytate (Solco-Phytate, Solco Ltd., Basle, Switzerland). The activity was 52–81 MBq and imaging was started 3–5 min after the injection. The second injection of ^{99m}Tc -macroaggregated albumin (Solco-MAA) was performed after the liver scan; the activity was 93–111 MBq and the imaging started 1–2 min after the injection with the patient lying supine in the same position during all these images. The whole procedure took 15–20 min and no movement artifacts were observed in these patients. The subtraction results were assessed iteratively by using scaling factors, and according to previous experience. They were considered positive only when appropriate quantitative tumor/background ratios (TBR) were recorded. The subtraction calculations and their relations to phantom measurements are described elsewhere (39). The tumor-to-background ratios were calculated using ROI-technique.

Other investigations. The following imaging methods were used in most patients for verification of RIL findings. Total body and brain CT were performed with Somatom DR 1 (Siemens), and ultrasound of upper abdomen with Sonoline 1 (Siemens) with a 5 MHz sector scanner. Chest and bone radiographs were taken in cases of bone pain or positive bone scintigraphy. The antibody scans and radiographic images were interpreted independently by two experienced observers (one specialist in nuclear medicine and one radiologist). The clinical information and patient records were analyzed by an oncologist. Mediastinal and pleural lesions were studied by CT and chest x-rays, and pleural effusions were examined by cytology. Several lymph node metastases were verified by needle biopsy (cytology). Cutaneous metastases were confirmed by biopsy (histology). The immunohistochemical stainings were performed as described earlier (40), similarly some paraffin sections of patient tumors were stained for BW 431/31, as well as for BW 431/26 and ZCEA₁.

Results

^{99m}Tc -anti-CEA. Part of data obtained from ^{99m}Tc -labeled anti-CEA in 12 patients has been reported elsewhere (40). Twelve of 16 with suspected or known lung cancer had positive immunoscintigrams; 19 to 25 lesions could be detected by RIL. There were 5 false positive and 2 true negative findings. The blood pool activity was rather high at 24 h; the biological half-life was 23.3 h, and the effective half-life 4.7 h (39). All the examined tumor sections (from 7 patients) were immunohistochemically positive for BW 431/26.

^{111}In -anti-CEA. Twenty-seven of 28 lung cancer patients had positive immunoscintigrams at the site of the primary tumor; two primary tumors had been operated radically before immunoscintigraphy, and in one primary tumor the finding was negative. A summary of the scintigraphy results is presented in the Table. In three cases, brain metastases, visualized in planar images, were better delineated

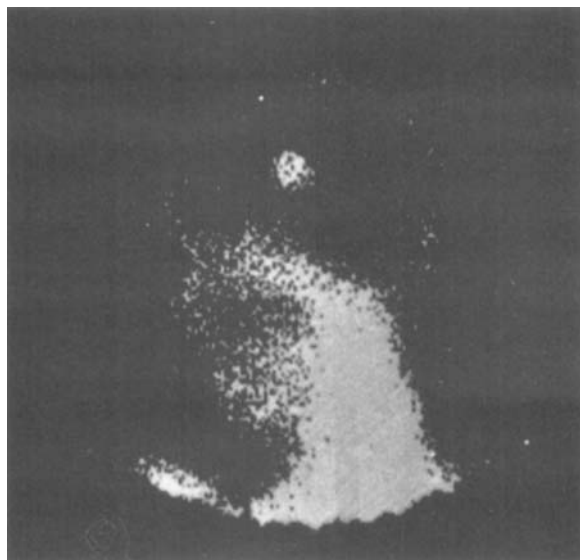


Fig. 1. Brain metastasis of lung cancer visualized by radioimmunoscintigraphy (BW 431/31).

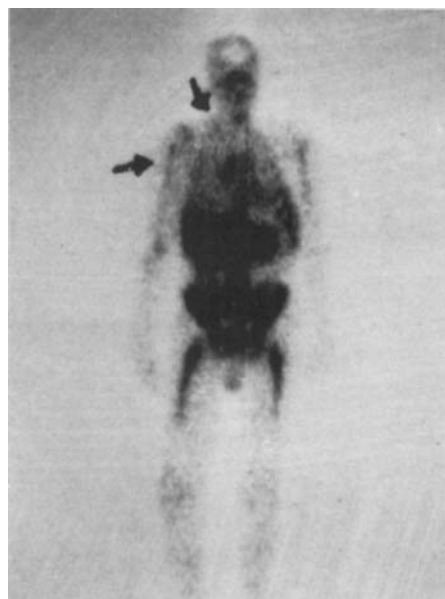


Fig. 2. Whole-body radioimmunoscan (BW 431/31) demonstrating primary squamous cell cancer in right lung, and a large supraclavicular lymph node metastasis.

with SPECT. Fig. 1 demonstrates a brain metastasis detected by RIL; the size of the tumor on CT was approximately 3 cm in diameter (patient No. 17, Table). In Fig. 2 a whole-body scan at 24 h is presented, demonstrating a primary squamous cell cancer in the right lung, and a large supraclavicular lymph node metastasis (patient No. 6, Table). In Fig. 3 a skeletal lesion is presented, which turned out to be a metastasis, and it was not detected by other imaging modalities (x-rays and bone scintigraphy,

Table

Patient characteristics, results of ¹¹¹In-anti-CEA immunoscintigraphy (IS) and other examination methods. TNM staging according to ref. (63)

Patient Age/Sex	Hist. diagn	Primary staging	Prim. tumor	Other lesions in IS scans	S-CEA $\mu\text{g/l}$	Verification methods	No. of lesions
1 52/F	AC	T3N2M0	pos	mediastinum	47	CT, brsc	2
2 67/M	SCC	T3N2M1	pos	pleura, brain, bone	7.2	CT, brsc, US	3**
	SCC	T2N0M1	pos	pleura, bone	3.2	obd, CT, BS	9
4 63/M	AC	T2N0M0	pos	bone	<3	CT, BS, x-ray	2
5 55/F	AC	T3N0M0	pos	pleura, brain, bone, skin, lung	168	obd, CT, BS	9
6 77/M	SCC	T2N1M0	pos	mediastinum, lnn	<3	CT, fnac	2
7 43/M	AC	T3N1M0	pos	mediastinum, pleura	<3	CT, brsc, cyt	3
8 68/M	SCC	T3N2M1	pos	mediastinum, pleura, lnn	<3	CT, brsc	3
9 49/M	SCC	T3N2M0	pos	mediastinum, pleura, lnn, thyroid, colon, liver, bone	13.6	obd, CT, BS, US	11**
10 60/F	AC	T3N0M1	pos	mediastinum, lnn	14.6	CT, brsc, fnac	4**
11 59/M	SC	T2N0M0	pos	bone	nd	CT, brsc, MRI	3**
12 64/F	SCC	T3N0M0	pos	mediastinum, bone, colon	nd	CT, BS, US	4
13 55/F	AC	T3N1M0	pos	—	nd	CT, BS, US	1
14 70/M	SCC	T3N1M1	pos	brain, kidney, bone	nd	CT, brsc, BS	6
15 60/M	Ana	T3N0M1	pos	lnn, bone, liver	1115	CT, brsc, BS, fnac	6
16 61/M	SCC	T3NXM1	pos	brain, bone	nd	CT, brsc, BS	4
17 73/M	SCC	T2N0M0	neg*	brain, bone	3.1	CT, BS	3
18 67/M	SCC	T2N0M0	pos	mediastinum, lnn, bone	nd	CT, BS	5
19 65/M	SCC	T3N1M0	pos	mediastinum, bone	nd	CT, brsc, BS	4
20 64/M	SCC	T2N2M0	pos	brain	3.6	CT, brsc	2**
21 61/M	SCC	T3N0M1	neg*	mediastinum	<3	CT	1
22 65/M	SCC	T3N1M0	neg	—	nd	CT	0
23 68/F	SCC	T2N1M0	pos	bone	nd	CT, BS	2
24 67/M	AC	T2N2M0	pos	bone	nd	CT, BS	2
25 63/M	SCC	T3N2M0	pos	—	<3	CT, brsc	1
26 57/M	AC	T3N2M0	pos	mediastinum, bone	nd	CT, brsc, fnacs	3
27 65/M	SCC	T3N1M0	pos	colon	<3	CT	2
28 62/M	SCC	T3NXMX	pos	bone	nd	brsc, x-ray	5
29 67/M	AC	T3N2M0	pos	mediastinum	nd	CT	2
30 73/M	SCC	T1N0M0	pos	bone	nd	CT	3

* = primary tumor operated ** lesions not detected by IS: No. 2 mediastinal lnn, right adrenal (CT); No. 9 3 lesions in autopsy; No. 10 left adrenal (CT); No. 11 brain (CT, MRI); No. 20 mediastinal lnn (CT)

Abbreviations: AC = adenomatous carcinoma, Ana = anaplastic carcinoma, brsc = bronchoscopy, BS = bone scintigraphy, CT = computerized tomography, cyt = cytology from pleural effusate, fnac = fine needle aspiration cytology, IS = immunoscintigraphy, lnn = lymph node, nd = not done, obd = autopsy, SC = small cell carcinoma, SCC = squamous cell carcinoma, US = ultrasonography, x-ray = roentgenograph

patient No. 24, Table). Altogether 6 lesions, previously unknown, were found to represent metastases located in bone/bone marrow. In one case, brain SPECT was negative, whereas another SPECT study revealed multiple metastases (Fig. 4, patient No. 5, Table). Two patients had liver metastases detected only after subtraction. In general, detection of thoracic lesion was improved by pulmonary perfusion subtraction. This type of subtraction also gave information on pulmonary perfusion. When the regional lung perfusion was impaired, the uptake in the lung tumors was often lower than in tumors situated in areas with normal perfusion. In some cases excellent visual information was obtained in planar images, as shown in Fig. 5. In the spot image pleural effusion, supraclavicular lymph node, rib involvement and the primary squamous cell cancer are clearly visualized (patient No. 18, Table).

The tumor-to-background ratios varied from 1.6 to 2.9 at 20–28 h and from 1.2 to 4.1 at 49–77 h respectively. The TBRs varied from 1.4 to 4.1 in adenocarcinomas and from 1.2 to 3.5 in squamous cell carcinomas. There was no statistical difference in the TBRs between these malignancies. In general, the TBRs were slightly higher in later images. The tumor delineation too was usually better in later images even though all tumors were visualised in both imaging sessions. The TBRs were calculated for primary tumors in non-subtracted images (Table). In the two cases without visualized primary tumors the TBRs derive from metastatic sites. There was a difference in the immunohistochemical stainability between adenomatous and squamous cell carcinomas. All adenomatous cancers showed slightly stronger reaction, a phenomenon which can be seen in Fig. 6.

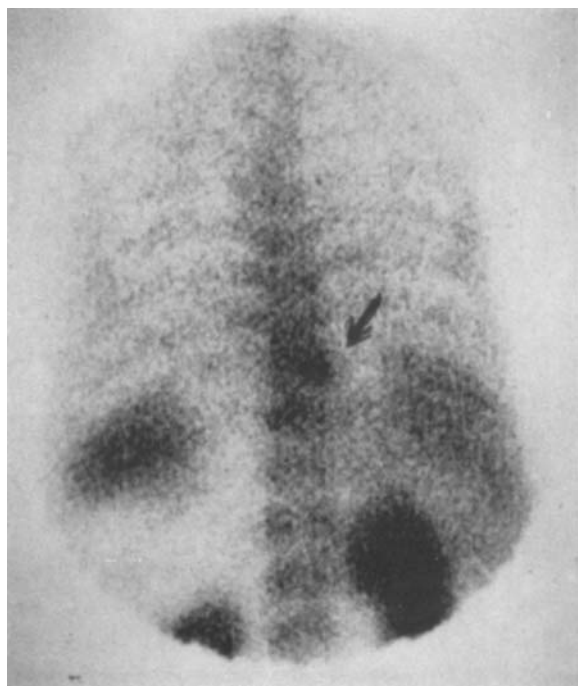


Fig. 3. A bone metastasis detected by radioimmunoscintigraphy (BW 431/31) but not by conventional bone scintigraphy.

The serum CEA concentration did not correlate with the number of lesions detected ($r = 0.09$, $n = 16$). Nor did the counts/pixel at the tumor sites correlate with the serum CEA concentration ($r = 0.14$, $n = 61$).

Discussion

The present study shows that lung cancer can frequently be detected with monoclonal anti-CEA antibodies. Most non-small cell lung cancers react with CEA immunohistochemically (38, 41–48). With this antibody, intense immunohistochemical staining is obtained both in squamous cell and adenomatous cancer cells (Fig. 6) in contrast to normal lung tissue. CEA is a tumor-associated antigen (49), also present *in vivo* in colorectal (50–54), breast (36, 54, 55), urinary bladder (56) and medullary thyroid cancers (57), tumors that—according to observations made by us and others (50–57)—can be visualized with the radioantibody used in the present study.

All lesions except those identified with subtraction were visualized already in the first image. However, the uptake was generally higher in the late images, when the circulating antibody-antigen complexes had been eliminated by the reticuloendothelial system, demonstrating the specific nature of the antigen-antibody binding. The late images (2–3 d) are of special importance due to less disturbing effect by the blood pool and the normal tissues which especially facilitates the visualization of pulmonary and mediastinal lesions.

One of the problems in staging of lung cancer is mediastinal involvement (58), since both CT (59) and MR (60) has rather low sensitivity for detection of such involvement. Immunoscintigraphy was positive in 11 of our 13 cases with mediastinal lesions observed in CT. In the mediastinum the lesions had to be relatively large in order to be visualized in the antibody scan. The TBRs were on average higher in adenocarcinomas than in epidermoid cancers. This was not an unexpected finding because immunohistochemically adenocarcinomas react more strongly with anti-CEA antibodies than squamous cell cancers (38, 41–45). This anti-CEA antibody method produced quite high TBRs and 96% of the primary lung cancers were visualized. It is possible that the accumulation of the radioactive antibody fragment observed in the present study is partly due to non-specific mechanism as weak uptake in non-stainable small cell lung cancer also observed.

We also detected 6 previously unknown lesions, subsequently verified to be metastases of lung cancer, showing the RIL can give information not attainable with the other radiological methods at the time of the investigation. For the detection of skeletal metastases bone scintigraphy was performed and false positive findings were obtained in 4 patients (11 lesions).

The clinical utility of radiolabeled anti-CEA-antibodies is not yet established, since the lesions detected were usually relatively large and in most cases also detected with other methods. Importantly, the sensitivity of immunoscintigraphy was quite high and with this single modality we were able to detect lung cancer metastases in 80% of the patients diminishing the need for other radiological investigations. In a study of 63 patients (26) an overall detection rate of 90% was reported. The best accuracy (86%) was observed in M1 disease.

The lesions seen in the antibody scans were in general quite large ($>2\text{cm}$) as measured by different radiologic methods. No solitary lesion smaller than one cm could be detected in the antibody scans in any organ. The lesions in pleura, mediastinum and pericardium were better delineated in subtraction images than in unprocessed planar immunoscintigraphic images. The specificity of the method was quite high and better than that of other radiological methods.

Diffuse uptake of activity was sometimes observed, especially in the lung area, probably partly due to malignant pleural effusions. Some of the pleural effusions were CEA positive, although no malignant cells could be detected. CEA as a serum marker has diagnostic and prognostic significance in lung cancer, also in monitoring the quality of operation (61, 62).

We conclude that detection of lung lesions by immunoscintigraphy can be improved by subtraction techniques, and that immunoscintigraphy is a potentially useful method for staging of non-small cell lung cancer, although more experience is needed for an ultimate assessment of its clinical value.

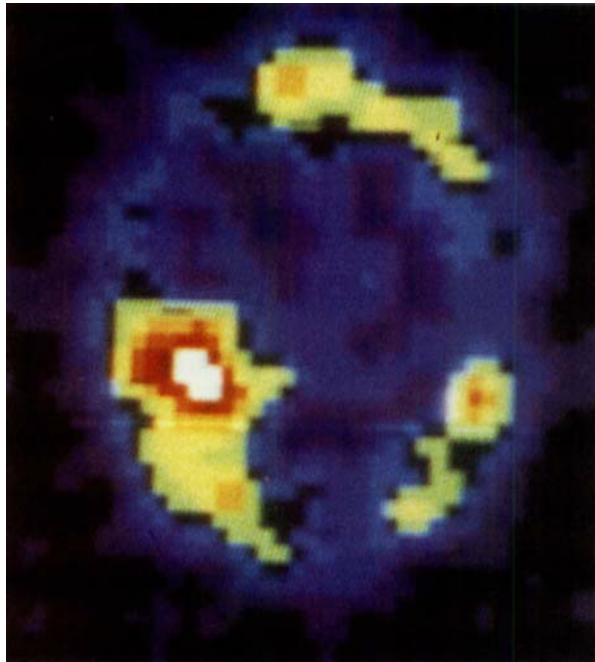


Fig. 4. A SPECT study (BW 431/31) demonstrating multiple brain metastases.

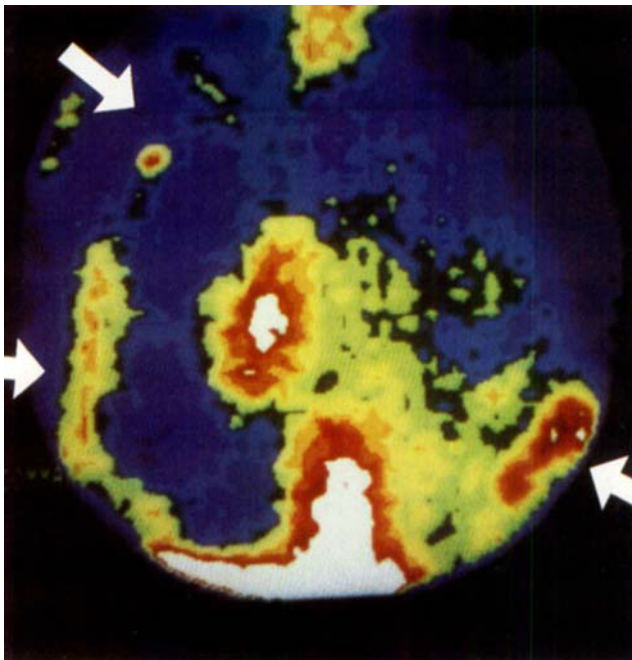
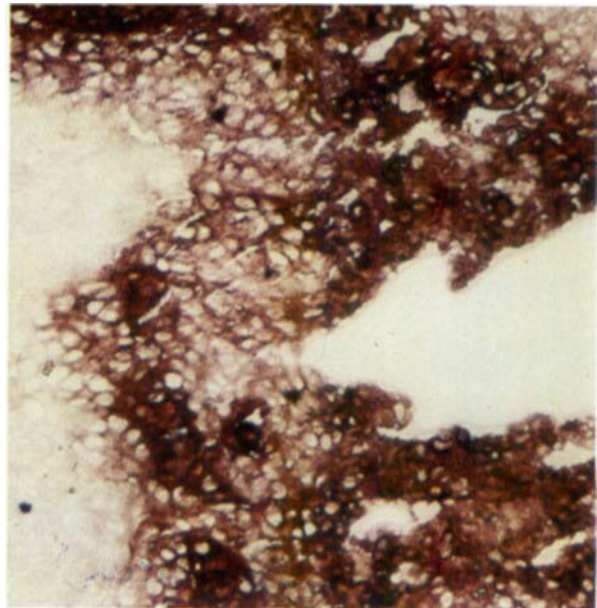


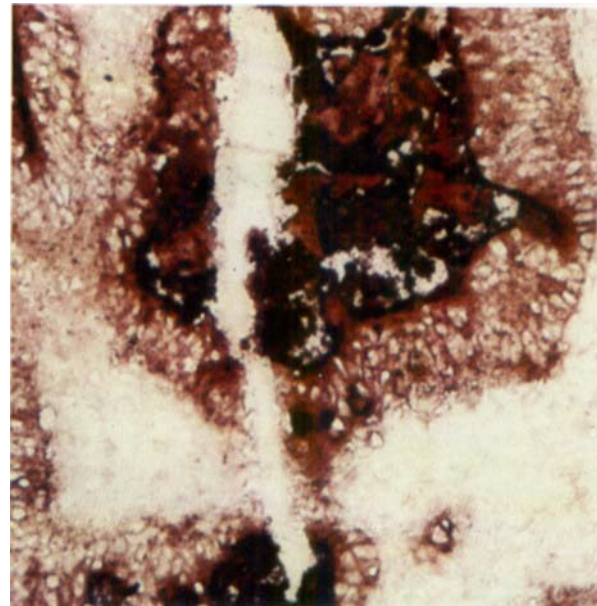
Fig. 5. RIL (BW 431/31) demonstrating a primary squamous cell cancer in right lung, and a small supraclavicular lymph node metastasis, pleural effusion and rib metastasis.

ACKNOWLEDGEMENTS

The authors are grateful to Dr. K. Bosslet and Dr. H. Sedlacek (Behringwerke AG, Marburg, Germany) for providing figures, presenting immunohistochemical stainings. The authors are



a)



b)

Fig. 6. Immunohistochemical staining (BW 431/31) of lung cancer. a) squamous cell carcinoma and b) adenocarcinoma.

also indebted to Behringwerke AG for supplying monoclonal antibodies and for their help in HAMA measurements, Drs. L. Seidel and H. Moritz are personally acknowledged for their assistance.

REFERENCES

1. Mann H. CT in the management of lung cancer. *Semin US CT MR* 1988; 9: 40-52.
2. Webb WR. MR imaging in the evaluation and staging of lung cancer. *Semin US CT Mr* 1988; 9: 53-66.

3. Stiglbauer R, Schurawitzki H, Klepetko W, et al. Contrast-enhanced MRI for the staging of bronchogenic carcinoma: comparison with CT and histopathologic staging—preliminary results. *Clin Radiol* 1991; 44: 293–98.
4. McCloud TC, Bourgoin PM, Greenberg RW, et al. Bronchogenic carcinoma: analysis of staging the mediastinum with CT by correlative lymph node mapping and sampling. *Radiology* 1992; 182: 319–25.
5. Musset D, Grenier P, Carette MR, et al. Primary lung cancer staging: prospective comparative study of MR imaging with CT. *Radiology* 1986; 160: 677–11.
6. DeMeester TR, Golomb HM, Kirchner P. The role of gallium-67 scanning in the clinical staging and preoperative evaluation in patients with carcinoma of the lung. *Ann Thorac Surg* 1979; 28: 451–7.
7. Bekerman C, Hoffer PB, Bitran JD. The role of gallium-67 in the clinical evaluation of cancer. *Semin Nucl Med* 1985; 15: 72–103.
8. Nieweg OE, Piers DA, Beekhuis H, Sluiter HJ, van der Wal AM, Woldring MG. ⁵⁷Co-bleomycin scintigraphy for the staging of lung cancer. *Cancer* 1989; 63: 1119–22.
9. Vorne M, Alanko K, Järvi K, et al. Comparison of gallium-67 citrate and technetium-99m glucoheptonate in the evaluation of pulmonary malignancies. *J Nucl Med* 1987; 28: 442–6.
10. Baum RP, Lorenz M, Hör G. Radioimmunszintigraphie bei kolorektalen Karzinomen—Stellenwert in der Rezidivdiagnostik nach 2 Jahren klinischer Erfahrung. *Der Nuklearmediziner* 1987; 10: 219–34.
11. Goldenberg DM, DeLand FH. Review. History and status of tumor imaging with radiolabeled antibodies. *Journal of Biological Response Modifiers* 1982; 1: 121–36.
12. O'Grady LF, DeNardo G, DeNardo S. Radiolabelled monoclonal antibodies for the detection of cancer. *Am J Physiol Imaging* 1986; 1: 44–53.
13. Larson SM. Cancer imaging with monoclonal antibodies. In DeVita VT Jr, Hellman S, Rosenberg SA, eds. *Important advances in oncology* 1986. J. P. Lippincott Co, 1986: 233–49.
14. Goodwin DA, Meares CF, McCall MJ, McTigue M, Chaovapong W. Pretargeted immunoscintigraphy of murine tumors with indium-111-labeled bifunctional haptens. *J Nucl Med* 1988; 29: 226–34.
15. Pimm MV, Fells HF, Perkins AC, Baldwin RW. Iodine-131 and indium-111 labelled avidin and streptavidin for pretargeted immunoscintigraphy with biotinylated anti-tumour monoclonal antibody. *Nucl Med Commun* 1988; 9: 931–41.
16. DeNardo SJ, Warhoe KA, O'Grady LF, et al. Radioimmunotherapy for breast cancer: treatment of a patient with I-131 L6 chimeric monoclonal antibody. *Int J Biol Markers* 1991; 6: 221–30.
17. LoBuglio AF, Wheeler A, Leavitt RD, et al. Clinical trial of chimeric mouse-human monoclonal antibody in man. *Journal of Biological Response Modifiers* 1989; 8: 309.
18. Blumenthal RD, Sharkey RM, Snyder D, Goldenberg DM. Reduction of anti-antibody administration of the radiotoxicity associated with I-131-labeled antibody to carcinoembryonic antigen in cancer radioimmunotherapy. *J Natl Cancer Inst* 1989; 81: 194–9.
19. Goldenberg DM, Anderson LD, Sharkey RM, Ford E. Anti-antibody enhancement of iodine-131 anti-CEA radioimmunodetection in experimental and clinical studies. *J Nucl Med* 1987; 28: 1604–10.
20. Stickney DR, Anderson LD, Slater JB, et al. Bifunctional antibody: a binary radiopharmaceutical delivery system for imaging colorectal carcinoma. *Cancer Res* 1990; 51: 6650–5.
21. Goodwin DA, Meares CF, McTigue M, et al. Pretargeted immunoscintigraphy: effect of hapten valency on murine tumor uptake. *J Nucl Med* 1992; 33: 2006–13.
22. Riva P, Moscatelli G, Paganelli G, Benini S, Siccardi A. Antibody-guided diagnosis: An Italian experience on CEA-expressing tumours. *Int J Cancer* 1988; (Suppl. 2): 114–20.
23. Liewendahl K, Kairemo K, Brownell A-L, Mäntylä M. Experience with In-111-labelled anti-CEA antibody for imaging lung cancer metastases. *Nucl Med* 1989; 25(Suppl): 353–6.
24. Happ J, Baum R, Frohn J, et al. Immunszintigraphie mit ¹¹¹In-DTPA-markierten monoklonalen Antikörpern: Vergleich zwischen ECT und planarer Szintigraphie. *Nucl Med* 1987; 26: 258–62.
25. Leitha T, Walter R, Schlick W, Dudczak R. ^{99m}Tc-anti-CEA radioimmunoscintigraphy of lung adenocarcinoma. *Chest* 1991; 99: 14–9.
26. Buccheri G, Biggi A, Ferrigno D, et al. Imaging lung cancer by scintigraphy with indium 111-labeled F(ab')₂ fragments of the anticarcinoembryonic antigen monoclonal antibody F023C5. *Cancer* 1990; 70: 749–59.
27. Endo K, Kamma H, Ogata T. Radiolocalization of xenografted human lung cancer with monoclonal antibody 8 in nude mice. *Cancer Res* 1987; 47: 5427–32.
28. Dazord L, Bourel D, Martin A, et al. A monoclonal antibody (Po66) directed against human lung squamous cell carcinoma. Immunolocalization of tumour xenografts in nude mice. *Cancer Immunol Immunother* 1987; 24: 263–68.
29. Stya M, Wahl RL, Natale RB, Beierwaltes WH. Radioimmunoinaging of human small cell lung carcinoma xenografts in nude mice receiving several monoclonal antibodies. *NCI Monogr* 1987; 3: 19–23.
30. Zimmer AM, Rosen ST, Spies SM, et al. Radioimmunoinaging of human small cell lung carcinoma with I-131 tumor specific monoclonal antibody. *Hybridoma* 1985; 4: 1–11.
31. Sugiyama Y, Chen FA, Takita H, Bankert RB. Selective growth inhibition of human lung cancer cell lines bearing a surface glycoprotein gp 160 by ¹²⁵I-labeled anti-gp 160 monoclonal antibody. *Cancer Res* 1988; 48: 2768–73.
32. Waibel R, O'Hara CJ, Smith A, Stahel RA. Tumor-associated membrane sialoglycoprotein on human small cell lung carcinoma identified by the IgG_{2a} monoclonal antibody SWA 20. *Cancer Res* 1988; 48: 4318–25.
33. Mulshine JL, Keenan AM, Carrasquillo JA, et al. Immunolymphoscintigraphy of pulmonary and mediastinal lymph nodes in dogs: a new approach to lung cancer imaging. *Cancer Res* 1987; 47: 3572–6.
34. Chan SYT, Evan GI, Ritson A, Watson J, Wraight P, Sikora K. Localisation of lung cancer by a radiolabelled monoclonal antibody against the c-myc oncogene product. *Br J Cancer* 1986; 54: 761–9.
35. Halpern SE, Dillman RO. Review. Problems associated with radioimmunodetection and possibilities for future solutions. *Journal of Biological Response Modifiers* 1987; 6: 235–62.
36. Kairemo KJA. Immunolymphoscintigraphy with Tc-99m-labeled monoclonal antibody (BW 431/26) reacting with carcinoembryonic antigen in breast cancer. *Cancer Res* 1990; 50: 949S–54S.
37. Schwarz A, Steinsträsser A. A novel approach to ^{99m}Tc-labeled monoclonal antibodies (abstract). *J Nucl Med* 1987; 28: 721.
38. Bosslet K, Lüben G, Schwarz A, et al. Immunohistochemical localization and molecular characteristics of three monoclonal antibody-defined epitopes detectable on carcinoembryonic antigen (CEA). *Int J Cancer* 1985; 36: 75–84.

39. Kairemo KJA, Kiuru AJ, Heikkonen JJ. Image subtraction analysis with technetium-99m labeled monoclonal antibody and colloid for evaluation of liver lesions; phantom measurements and patient studies. *Acta Oncol* 1993; 32: 763-9.
40. Aronen HF, Paavonen T, Heikkonen J, et al. Imaging of non-small cell lung cancer with Tc-99m-labeled monoclonal anti-CEA antibody with a comparison to immunohistochemistry. *Antibody Immunoconjugates and Radiopharmaceuticals*: 1991; 4: 569-75.
41. Gatter KC, Abdulaziz Z, Beverley P, et al. Use of monoclonal antibodies for the histopathological diagnosis of human malignancy. *J Clin Pathol* 1982; 35: 1253-67.
42. Lozowski W, Hajdu SI. Cytology and immunocytochemistry of bronchioloalveolar carcinoma. *Acta Cytol* 1987; 31: 717-25.
43. Gosh AK, Gatter KC, Dunnill MS, Mason DY. Immunohistological staining of reactive mesothelium, mesothelioma, and lung carcinoma with a panel of monoclonal antibodies. *J Clin Pathol* 1987; 40: 19-25.
44. Harach HR, Skinner M, Gibbs AR. Biological markers in human lung carcinoma: an immunopathological study of six antigens. *Thorax* 1983; 38: 937-41.
45. Sun NCJ, Edgington TD, Carpentier CL, McAfee W, Terry R, Bateman J. Immunohistochemical localization of carcinoembryonic antigen (CEA), CEA-S, and nonspecific cross-reacting antigen (NCA) in carcinomas of lung. *Cancer* 1993; 52: 1632-41.
46. Cuttita F, Rosen S, Gazdar AF, Minna JD. Monoclonal antibodies which demonstrate specificity for several types of human lung cancer and neuroblastoma. *Proc Natl Acad Sci USA* 1981; 78: 4591-4.
47. Espinoza CG, Balis JU, Saba SR, Paciga JE, Shelley SA. Ultrastructural and immunohistochemical studies of bronchiolo-alveolar carcinoma. *Cancer* 1984; 54: 2182-9.
48. Dulmet-Brender E, Jaubert F, Huchon G. Exophytic endobronchial epidermoid carcinoma. *Cancer* 1986; 57: 1358-64.
49. Martin EW, Kibbey WE, DiVecchia L, Anderson G, Catalano P, Minton JP. Carcinoembryonic antigen—Clinical and historical aspects. *Cancer* 1976; 37: 62-81.
50. Lind P, Lechner P, Arian-Schad K, et al. Anti-carcinoembryonic antigen immunoscintigraphy (technetium 99m-monoclonal antibody BW 431/26) and serum CEA levels in patients with suspected primary and recurrent colorectal carcinoma. *J Nucl Med* 1991; 32: 1319-25.
51. Hertel A, Baum RP, Auerbach B, Herrmann A, Hör G. Klinische Relevanz humaner Anti-Maus-Antikörper (HAMA) in der Immunszintigraphie. *Nucl Med* 1990; 29: 221-7.
52. Baum RP, Hertel A, Lorenz M, Schwarz A, Encke A, Hör G. 99Tcm-labelled anti-CEA monoclonal antibody for tumour immunoscintigraphy: first clinical results. *Nucl Med Commun* 1989; 10: 345-52.
53. Bock E, Becker W, Scheele J, Wolf F. Diagnostic accuracy of ^{99m}Tc-anti-CEA immunoscintigraphy in patients with liver metastases from colorectal carcinoma. *Nucl Med* 1992; 31: 80-3.
54. Leitha T, Baur M, Steger G, Dudczak R. Anti-CEA-Immunszintigraphie in der postoperativen Nachsorge von Tumorpacienten. Differenzierter Einsatz verschiedener monoklonaler Antikörperpräparationen. *Wien Klin Wochenschr* 1990; 102: 503-9.
55. Lind P, Smola P, Lechner P, et al. The immunoscintigraphic use of Tc-99m-labelled monoclonal anti-CEA antibodies (BW 431/26) in patients with suspected primary, recurrent and metastatic breast cancer. *Int J Cancer* 1991; 47: 865-9.
56. Kanokogi M, Becht E, Benz P, Ziegler M, Ikoma F, Oberhausen E. Carcino-embryonales Antigen (CEA) beim Harnblasenkarzinom; Eine immunhistochemische und immunszintigraphische Untersuchung. *Aktuelle Urologie* 1990; 21: 251-8.
57. Berche C, Mach J-P, Lumbroso J-D, et al. Tomoscintigraphy for detecting gastrointestinal and medullary thyroid cancers: first clinical results using radiolabeled monoclonal antibodies against carcinoembryonic antigen. *Br Med J* 1982; 285: 1447-51.
58. Tsi GM, Friedman PH, Peters RM. American thoracic society: clinical staging of primary lung cancer. *Am Rev Respir Dis* 1983; 127: 659-64.
59. Staples CA, Müller NL, Miller RR, Evans KG, Nelems B. Mediastinal nodes in bronchogenic carcinoma: comparison between CT and mediastinoscopy. *Radiology* 1988; 167: 367-72.
60. Webb WR, Gatsonis C, Zerhouni EA, et al. CT and MR imaging in staging non-small cell bronchogenic carcinoma: report of the Radiologic Diagnostic Oncology Group. *Radiology* 1991; 178: 705-13.
61. Gail MH, Muenz L, McIntire K, et al. Multiple markers for lung cancer diagnosis: validation of models for localized lung cancer. *J Natl Cancer Inst* 1988; 80: 97-101.
62. Vincent RG, Chu TM, Lane WW, et al. Carcinoembryonic antigen as a monitor of successful surgical resection in 130 patients with carcinoma of the lung. *Progress in cancer research and therapy*, vol. 1. In: Muggia FM, Rosencweig M, eds. *Lung Cancer : Progress in therapeutic research*. New York: Raven Press 1979: 191-8.
63. UICC TNM classification of malignant tumours. Hermanek P, Sobin LH, eds. 4th ed. Berlin: Springer-Verlag, 1987.